

# Crystallization Behavior, Mechanical Properties, and Environmental Biodegradability of Poly( $\beta$ -hydroxybutyrate)/Cellulose Acetate Butyrate Blends

Tiezhu Wang,<sup>1</sup> Guoxiang Cheng,<sup>1</sup> Shihu Ma,<sup>1</sup> Zhijiang Cai,<sup>1,2</sup> Liguang Zhang<sup>1</sup>

<sup>1</sup>School of Materials Science and Engineering, Tianjin University, Tianjin 300072, China

<sup>2</sup>Bioactive Materials Key Laboratory of the Ministry of Education, Nankai University, Tianjin 300071, China

Received 28 February 2002; accepted 16 November 2002

**ABSTRACT:** The miscibility, crystallization behavior, tensile properties, and environmental biodegradability of poly( $\beta$ -hydroxybutyrate) (PHB)/cellulose acetate butyrate (CAB) blends were studied with differential scanning calorimetry, scanning electron microscopy, wide-angle X-ray diffraction, and polarizing optical microscopy. The results indicated that PHB and CAB were miscible in the melt state. With an increase in the CAB content, the degree of crystallinity and melting temperature of the PHB phase decreased, and this broadened the narrow processability window of

PHB. As the elongation at break increased from 2.2 to 7.3%, the toughness and ductility of PHB improved. From the degradation test, it could be concluded that degradation occurred gradually from the surface to the inside and that the degradation rate could be adjusted by the addition of the CAB content. © 2003 Wiley Periodicals, Inc. *J Appl Polym Sci* 89: 2116–2122, 2003

**Key words:** blends; miscibility; biodegradable

## INTRODUCTION

In the past 30 years, plastics have been used widely in many areas, but the environmental pollution brought by plastic wastes has been a serious problem. Research into degradable plastics, especially biodegradable ones, has become a focus of new material research. Bacterial poly( $\beta$ -hydroxybutyrate) (PHB) is well known as a thermoplastic aliphatic polyester. It has many advantages, such as biodegradability, biocompatibility, and optical activity. The homopolymer PHB and some copolymers are commercially available, and a number of applications have been developed in such fields as medicine, environmental science, and agriculture.<sup>1–3</sup> However, PHB is quite brittle because of its high crystallinity<sup>4,5</sup> and instability in the molten state, and this narrows its processability window.<sup>6,7</sup> All these factors greatly limit its applicability. It is possible to improve its impact resistance and processability through mixing with some other polymer. PHB has been used in blends with other polymers, such as poly(ethylene oxide),<sup>8–10</sup> poly( $\epsilon$ -caprolactone),<sup>11</sup> poly(lactic acid),<sup>12</sup> poly(vinyl acetate),<sup>13,14</sup> and poly(methyl methacrylate).<sup>15</sup>

Cellulose acetate butyrate (CAB) is one of the most important thermoplastic cellulose esters, and it can be biodegraded in a natural environment. CAB has a combination of a high melting temperature ( $T_m = 160^\circ\text{C}$ ) and a high glass-transition temperature ( $T_g \sim 113^\circ\text{C}$ ).<sup>16</sup> In this study, PHB was blended with CAB. In addition to using this type of cellulose ester in a classical thermoplastic application, we are seeking a means of making the best use of the degradable polyester PHB. We have also been interested in the relationship between the blend morphology and physical properties. The miscibility and thermal and viscoelastic properties of PHB/CAB blends have been reported previously.<sup>17–19</sup> For this article, the crystallization, morphology, and environmental biodegradability of PHB/CAB blends were investigated in detail.

## EXPERIMENTAL

### Materials

PHB was kindly supplied by Tianjin Tianlu Food Co., Ltd. (Tianjin, China; weight-average molecular weight =  $4.3 \times 10^5$  and weight-average molecular weight/number-average molecular weight = 1.49, as obtained by gel permeation chromatography in chloroform at  $30^\circ\text{C}$ ). CAB was purchased from the Wuxi Chemical Industry Institute (Wuxi, China; number-average molecular weight =  $3 \times 10^4$ ). The content of butyryl groups was 55%, and that of acetyl groups was 4%; the moisture content was about 2%, and the limiting inherent viscosity was 0.4–0.7 Pa s.

Correspondence to: G. Cheng (gxcheng@tju.edu.cn).

Contract grant sponsor: Natural Science Foundation of Tianjin; contract grant number: 003801111.

Contract grant sponsor: Youth Teacher Foundation of the Ministry of Education; contract grant number: 2002-123.

TABLE I  
Composition and Code of PHB/CAB Blends

	Blend composition PHB/CAB (w/w)								
	100/0	90/10	80/20	70/30	60/40	50/50	30/70	10/90	0/100
Code	PHB	PHB90	PHB80	PHB70	PHB60	PHB50	PHB30	PHB10	CAB

### Preparation of the blends

Weighed amounts of the two components were first mixed in an HL-28 smash machine (Shanghai Hailin Ltd., Shanghai, China). PHB/CAB blends were obtained by melt mixing at 170–180°C (according to the blend composition). The temperature was controlled precisely to minimize the thermal degradation of PHB. The blend compositions are denoted as weight percentages and are given in Table I.

### Differential scanning calorimetry (DSC)

A DSC-204 thermal analyzer (Netzsch Ltd., Germany) was used to study the thermal properties of the PHB/CAB blends. So that the influence of different thermal histories would be eliminated, the samples were first heated from room temperature to 200°C. After being held for 2 min at 200°C, they were rapidly quenched in liquid nitrogen to –100°C, and this was followed by heating from –100 to 200°C. A scan rate of 10°C/min was used throughout.

### Scanning electron microscopy (SEM)

The microscopic morphologies of the PHB/CAB blends were investigated with SEM (Hitachi X-650, Japan) at a magnification of 2000× at 20 kV. The samples were fractured in liquid nitrogen so that the surfaces would not be affected by external stress. For the morphological measurements, the samples were then coated with gold to provide conductive surfaces.

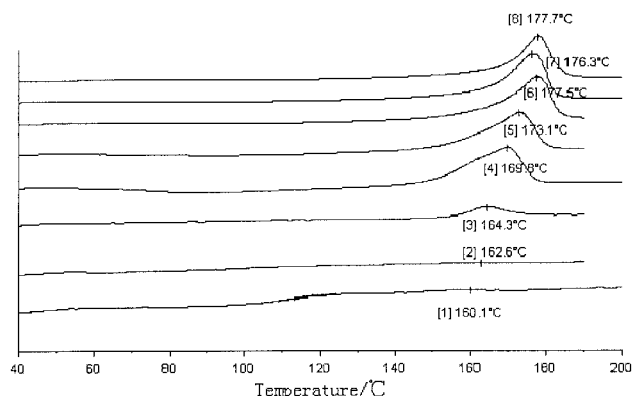


Figure 1 DSC thermograms of PHB/CAB blends: (1) CAB, (2) PHB10, (3) PHB30, (4) PHB50, (5) PHB60, (6) PHB80, (7) PHB90, (8) and PHB100.

### Polarizing optical microscopy (POM)

The shapes of the PHB spherulites in the blends were observed by POM. The samples were first heated to 190°C and were kept at this temperature for 1 min. The temperature was then lowered to room temperature, and PHB was allowed to crystallize. An Olympus polarizing optical microscope (Japan) equipped with a hot stage was used.

### Wide-angle X-ray diffraction (WAXD)

WAXD patterns of the PHB/CAB blends were recorded on a D/max-rB X-ray diffractometer (Rigaku Ltd., Japan). A nickel-filtered Cu K $\alpha$  X-ray beam with a pinhole graphite monochromator was used as the source. The wavelength of the X-ray beam was 0.1542 nm. The diffraction intensities of the films were measured in a 2 $\theta$  range of 10–25° at a scanning speed of 1° min<sup>-1</sup>.

### Mechanical tests

Dumbbell-shaped samples of PHB/CAB blends were used for tensile tests. The stress at break (MPa) and elongation at break (%) of the tested samples were measured with an M500-25KN universal testing machine (Testometric Co. Ltd., UK) at room temperature. The extension rate was 20 mm/min.

Standard samples of PHB/CAB blends were used for impact tests. The impact resistance was tested with a Chappy XCJ-500 impact tester (Ceast Ltd., Italy).

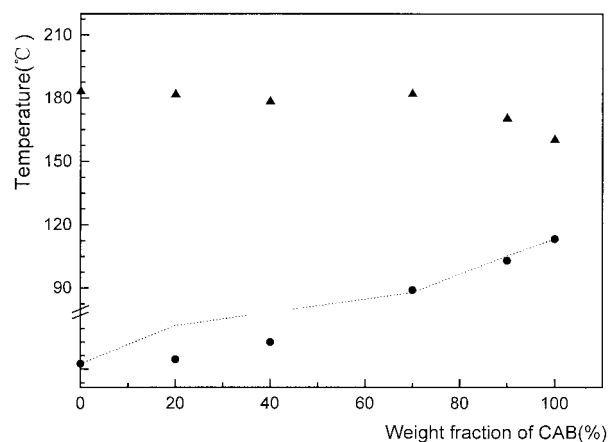


Figure 2 (▲)  $T_m$ 's, (●)  $T_g$ 's determined by DSC, and (–)  $T_g$ 's predicted with the equation for PHB/CAB blends.

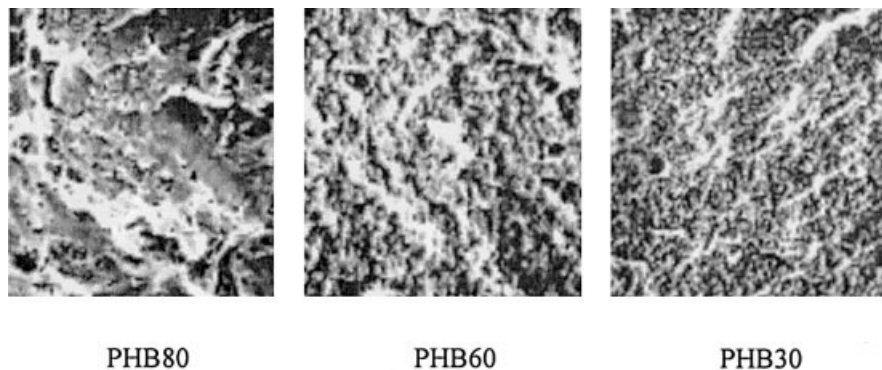


Figure 3 SEM micrographs of sections of PHB/CAB blends (2000 $\times$ ).

### Biodegradation tests

The hydrolytic degradation studies of the PHB/CAB blends were conducted at 25 $^{\circ}$ C in buffer solutions (pH 1.0 or 13.0) and in natural lake water (Youth Lake, Tianjin, China) stored in glass containers. The blends were taken out from the medium over a period of time and were washed with distilled water and subsequently dried at 100 $^{\circ}$ C for 1 h. The degradation rate was determined by the

ratio of the weight loss to the initial weight of the blend:

$$S = (W_0 - W_t)W_0$$

where  $S$  is the rate of weight loss and  $W_t$  and  $W_0$  are the weight after drying and the initial weight of the blends, respectively.

The microscopic appearance of the blends during degradation was also examined with SEM micrographs.

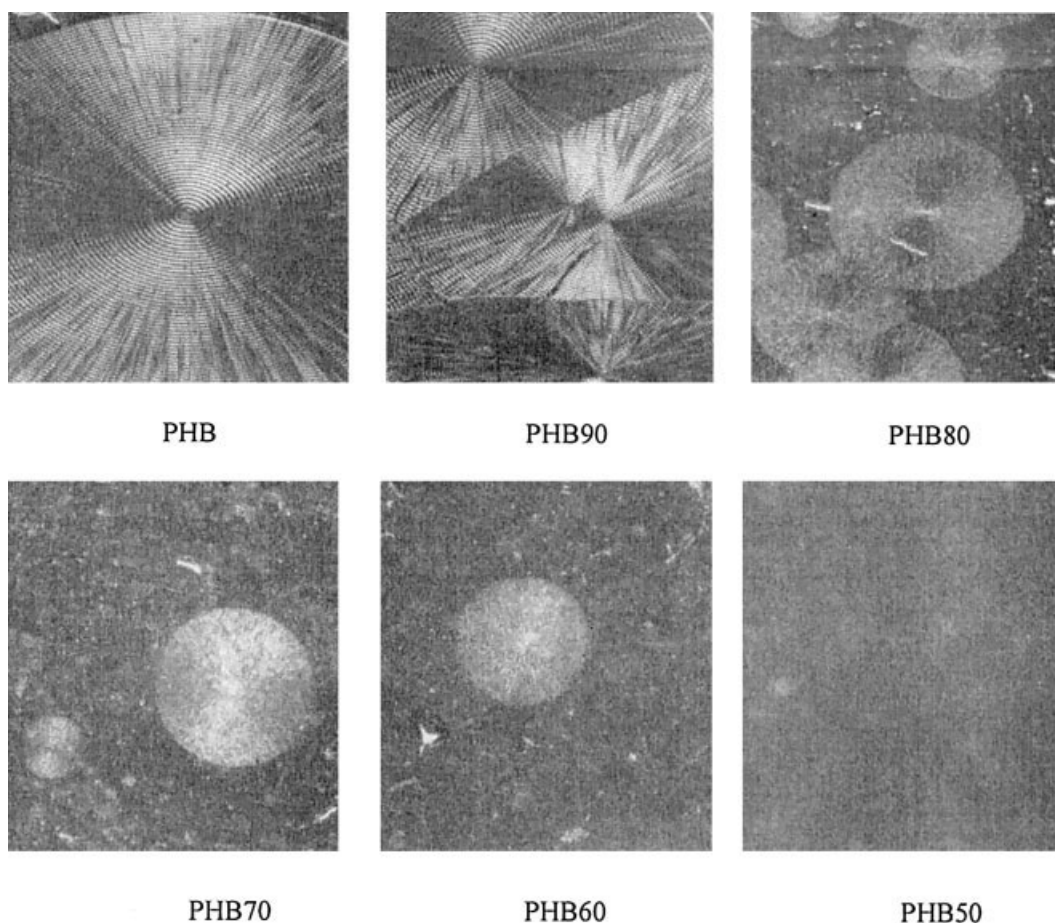


Figure 4 Optical micrographs of PHB spherulites of PHB/CAB blends (50 $\times$ ).

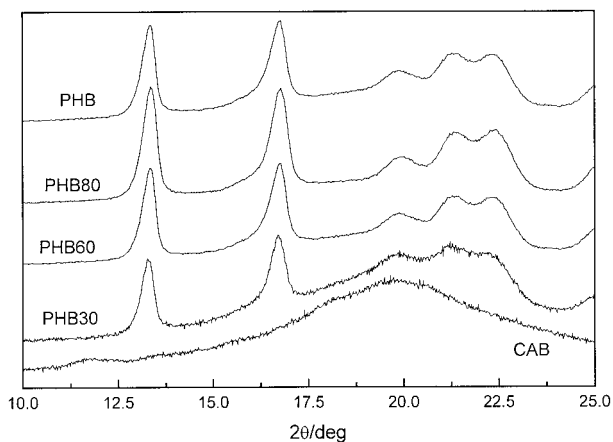


Figure 5 WAXD patterns of PHB/CAB blends.

RESULTS AND DISCUSSION

Thermal behavior and miscibility

The DSC thermograms of PHB/CAB blends are shown in Figure 1. When the content of PHB in the blends is greater than 30 wt %, an obvious melting peak can be seen in the DSC thermograms. With increasing CAB contents in the blends,  $T_m$  of the PHB phase decreases. The decrease in the observed  $T_m$  with an increase in the CAB content is what one would expect for a miscible system.<sup>20,21</sup>

$T_g$ 's of PHB/CAB blends are plotted in Figure 2 as a function of the composition. The curves drawn in Figure 2 correspond to Wood's equation:

$$T_g = (w_1T_{g1} + kw_2T_{g2}) / (w_1 + kw_2)$$

where  $w_1$  and  $w_2$  and  $T_{g1}$  and  $T_{g2}$  are the weight fractions and glass-transition temperatures of components 1 and 2, respectively.  $k$  is an adjustable empirical parameter ( $k = 0.70$  for the PHB/CAB blends).

When the PHB content is greater than 50 wt %, there is a slow but gradual increase in  $T_g$ . Meanwhile, when the PHB content is lower than 50 wt %, there is a strong dependence of the measured  $T_g$  on the composition. At first glance, the very small variation of  $T_g$  with composition for high levels of PHB can be taken

as evidence for phase separation in the amorphous zones. In fact, the trend in  $T_g$  is ascribed to the presence of two mobilization processes in a homogeneous blend. PHB and CAB are miscible in the melt state over the entire range of compositions, and this is consistent with previous reports.<sup>17</sup>

Microscopic appearance and spherulitic morphology

The morphology of the PHB/CAB blends observed by SEM is shown in Figure 3. When the content of CAB in the blends is low, there are many defects in the samples. With an increase in CAB, the defects decrease. The phase boundaries become more indistinct, and a very smooth texture can be observed. This alteration is supposed to arise from the drop of  $T_m$  of PHB and the broadening of the narrow processability window when CAB is blended with PHB. The  $T_m$  values of PHB and CAB become closer with an increase in CAB; this helps the formation of a homogeneous mixture, and the processability of PHB is improved. This improvement is enhanced with the increase in the CAB content.

As shown by the POM micrographs in Figure 4, PHB crystallizes according to a spherulitic morphology, shows a Maltese cross birefringent pattern, and exhibits concentric extinction bands. However, with an increase in the amorphous polymer CAB, the spherulites become small and imperfect, and the number of spherulites that can be observed decreases gradually. When the CAB content is greater than 50%, no spherulites can be found, and this is due to a homogeneous amorphous phase formed by PHB and CAB. Therefore, it can be concluded that when PHB is greater than 50%, the addition of CAB is conducive to the reduction of the PHB crystallinity and the improvement of the PHB toughness.

The WAXD patterns of PHB/CAB blends are shown in Figure 5. For pure PHB, two strong and sharp scattering intensity peaks are detected at  $2\theta = 13$  and  $17^\circ$ . Only very broad scattering intensity peaks are detected around  $2\theta = 20^\circ$  for pure CAB. With increased contents of CAB, the positions of the diffrac-

TABLE II  
Tensile Properties of PHB/CAB Blends

PHB/CAB blend	Tensile modulus (MPa)	Tensile strength (MPa)	Elongation at break (%)	Impact strength (kg/m <sup>2</sup> )
PHB	1679.2	25.703	2.169	20.2
PHB90	2288.3	26.796	2.2214	21.8
PHB80	1671.9	29.299	3.3386	32.4
PHB70	1192.6	20.391	2.0386	41.5
PHB60	1153.8	16.985	2.0457	57
PHB50	592.44	13.334	7.286	59
CAB	1018.7	5.5659	0.5886	7.5

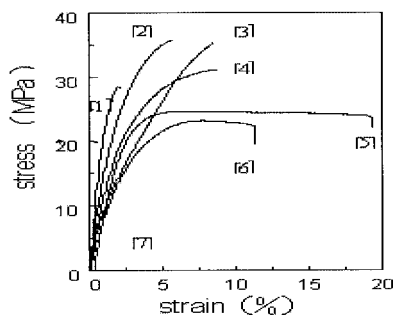


**Figure 6** Stress-strain curves of PHB/CAB blends: (1) PHB, (2) PHB90, (3) PHB80, (4) PHB70, (5) PHB60, (6) PHB50, and (7) CAB.

tion peaks change slightly, and this implies that the addition of CAB does not result in any change in the crystalline structure of PHB. However, the scattering intensity of PHB decreases remarkably. The reason suggested is that CAB molecules are trapped between the PHB lamellae, and this prevents the formation of PHB spherulites and brings about a decrease in the PHB crystallinity. This is consistent with the results obtained by DSC.

### Mechanical properties

The tensile strength, elongation at break, and impact strength are all improved by the addition of CAB, as shown in Table II. Pure PHB and CAB typically show brittle properties (Fig. 6). The addition of CAB improves the impact resistance of blends, and an obvious yield can be observed for the 60/40 and 50/50 blends, which show the characteristics of ductility. This result can be explained by the crystallinity of PHB being as high as 80%; therefore, the microcrystals connect to one another and form a continuous phase. Moreover, spherulites of PHB are much bigger than those of polypropylene. In this case, when the material is drawn, the big spherulites are easier to crack. The alteration of the molecular conformation is difficult because the movement of molecular segments is retarded by the continuous crystallization phase. All this results in the brittle property of PHB. CAB is a non-crystallizable polymer with a high  $T_g$  of about 113°C. PHB/CAB blends have been proven to be miscible for all ranges of compositions.<sup>22</sup> When the blends are crystallized at room temperature, which is much lower than  $T_g$  of CAB but higher than  $T_g$  of PHB, PHB molecules in the amorphous state are probably trapped by the glassy CAB environment. This reduces the crystallinity of PHB and also affects the regularity and continuity of the PHB crystalline phase with increasing contents of CAB. At this time, the molecular segments are easier to orient when PHB is drawn. The microfibers of CAB dispersed in the PHB crystallized phase can induce the production of silver streaks,

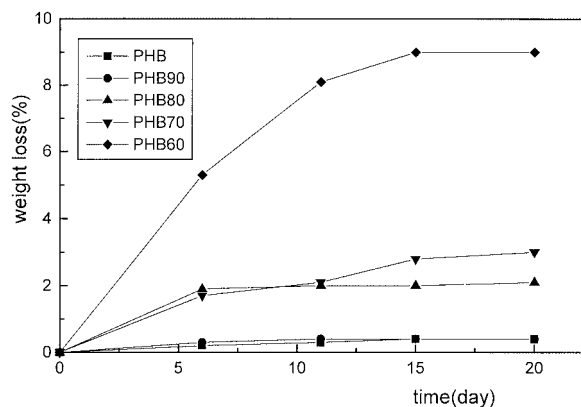


**Figure 7** Weight loss (%) of PHB/CAB blends in a pH 1 buffer solution.

which absorb most of the impacting energy for the impact experiment. Therefore, the toughness of the PHB material is improved.

### Biodegradability

PHB has two degradation mechanisms. One is hydrolysis in a sterile medium,<sup>23</sup> the other is enzyme degradation in a natural environment.<sup>24</sup>

#### Degradation in buffer solutions

Figures 7 and 8 show the degradation rates of PHB/CAB blends in buffer solutions of pH 1.0 and pH 13.0, respectively. The degradation rates of the same blends in acidic media are much slower than those in alkaline media. It can be concluded that the degradation of PHB/CAB blends is strongly influenced by the pH, as reported previously.<sup>25</sup> It is thought that the blends degrade by significantly different routes, depending on the pH of the surrounding medium. Neutral and acidic solutions produce more diffuse surface degradation, whereas degradation in alkaline solutions appears to be more aggressive, with specific sites of

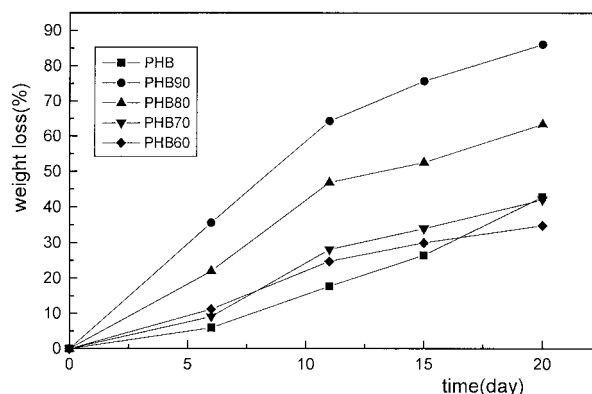


**Figure 8** Weight loss (%) of PHB/CAB blends in a pH 13 buffer solution.

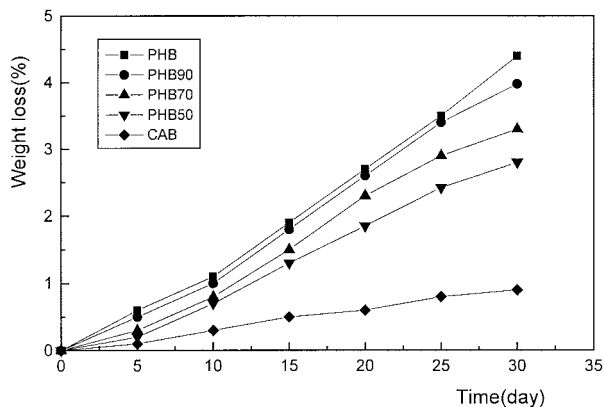


Figure 9 Weight loss (%) of PHB/CAB blends in natural water.

attack occurring that produce deep points of surface erosion.

However, the blending of CAB with PHB increases the degradation rates of blends in acidic and alkaline

media. In an acidic medium, increasing the CAB content accelerates the degradation, whereas in an alkaline medium, the degradation rate decreases with the CAB content increasing. For PHB, in acidic and neutral solutions, hydrolysis proceeds by a protonation process, followed by the addition of water and the cleavage of linkages. In an alkaline medium, hydroxyl ions are attached to the carbonyl carbon. The ester linkages are subsequently ruptured. This could explain the difference between the mass losses dependent on the pH.

Degradation in natural water

Figure 9 shows the degradation rate of PHB/CAB blends in natural water. The appearances of PHB, CAB, and PHB50 degradation in natural water are shown in Figure 10. CAB is a kind of cellulose mixed ester containing acetyl and butyryl groups. The substituents and steric hindrance in CAB prevent micro-

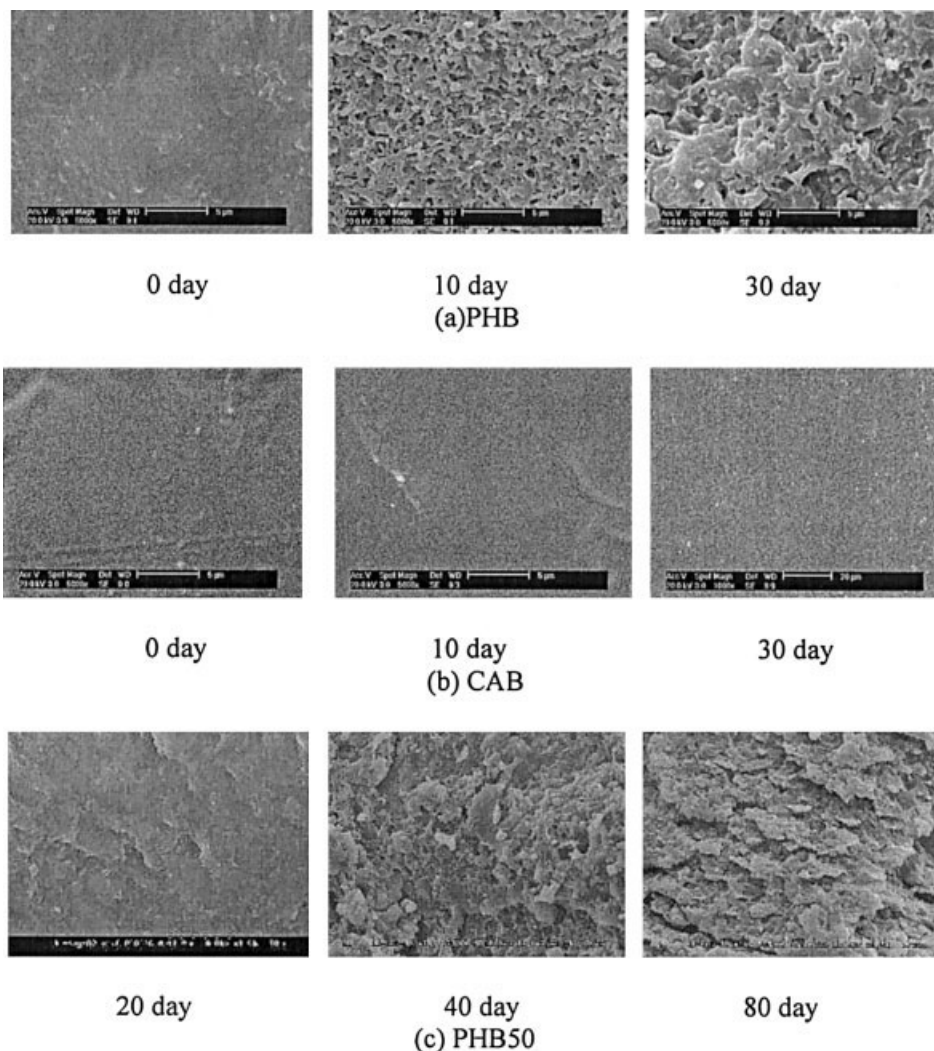


Figure 10 SEM micrographs of surfaces of (a) PHB, (b) CAB, and (c) PHB50 in water (5000×).

organisms from corroding the cellulose. Therefore, the degradation of CAB is much slower than that of PHB. The biodegradation of PHB proceeds from amorphous regions on the surface by microorganisms in natural water, and erosion develops gradually to the inside. With the prolongation of the biodegradation time, the blend surface becomes rougher and rougher, and many corrosive spots can be seen. As already mentioned, CAB and PHB are miscible in the melt state and can form a homogeneous mixture. The existence of CAB reduces the opportunity of PHB contacting the water. Therefore, the degradation rate of PHB50 blends is lower than that of the pure PHB.

### CONCLUSIONS

The results of DSC, SEM, POM, and WAXD indicate that PHB and CAB are miscible in the melt state. As CAB is blended with PHB,  $T_m$  of PHB decreases, and this influence is enhanced with the increase of the CAB content. The degree of crystallinity of PHB also decreases, but the processability and toughness are improved. The degradation rate of PHB in an acidic medium is much slower than that in an alkaline medium. In a natural environment, degradation occurs gradually from the surface to the inside. The degradation rates of blends can be adjusted by the CAB content.

### References

- Nicholas, J. C.; Colin, H. L. K. *Polymer* 1994, 35, 4595.
- Norma, G.; Chavati, R. *Polym Int* 1999, 48, 1202.
- Cai, Z. J.; Cheng, G. X. *J Funct Polym* 2001, 14, 355.
- Barham, P. J.; Kellar, A. *J Polym Sci Part B: Polym Phys* 1986, 24, 69.
- Koning, G. J. M.; Lemstra, P. J. *Polymer* 1994, 35, 4598.
- Howells, E. R. *Chem Ind* 1982, 8, 508.
- Hammand, T.; Liggat, J. J. In *Principles and Applications*; Scott, G.; Gilead D., Eds.; Chapman and Hall: New York, 1995; p 1.
- Avella, M.; Martuscelli, E.; Greco, P. *Polymer* 1991, 32, 1647.
- Avella, M.; Martuscelli, Z.; Raimo, M. *Polymer* 1994, 35, 4598.
- Choi, H. J.; Park, S. H.; Yoon, J. S.; Lee, H. S. *Polym Eng Sci* 1995, 35, 1636.
- Kim, B. O.; Woo, S. I. *Polym Bull* 1998, 41, 707.
- Zhang, L. L.; Chen, D. X. *Polymer* 1996, 37, 235.
- An, Y. X.; Li, L. X.; Dong, L. S.; Mo, Z. S.; Feng, Z. L. *J Polym Sci Part B: Polym Phys* 1999, 37, 443.
- Hay, J. N.; Sharma, L. *Polymer* 2000, 41, 5749.
- Lotti, N.; Pizzoli, M.; Ceccorulli, G.; Scandola, M. *Polymer* 1993, 34, 4935.
- Encyclopedia of Chemical Industry*; Chemical Industry: Beijing, China 1998; Vol. 17.
- Ceccorulli, G.; Pizzoli, M.; Scandola, M. *Macromolecules* 1993, 26, 6722.
- El-Shafee, E.; Saafd, G. R.; Fahmy, S. M. *Eur Polym J* 2001, 37, 2091.
- Pizzoli, M.; Scandola, M.; Ceccorulli, G. *Macromolecules* 1994, 27, 4755.
- Nishi, T.; Kwei, T. K.; Wang, T. T. *J Appl Phys* 1975, 46, 4157.
- Nishio, Y.; Haratani, T.; Takahashi, T.; Manley, R. S. *J Macromolecules* 1989, 22, 2547.
- El-Shafee, E.; Gamal, R. S.; Sherif, M. F. *Eur Polym J* 2001, 37, 2091.
- Mergaert, J.; Anderson, C.; Wouters, A.; Swings, J. *J Environ Polym Degrad* 1994, 2, 177.
- Yoshie, N.; Nakasato, K.; Fujiwara, M.; Kasuya, K.; Abe, H.; Doi, Y.; Inoue, Y. *Polymer* 2000, 41, 3227.
- Lauzier, C.; Revol, J. F.; Debzi, E. M. *Polymer* 1994, 35, 4156.